Title: Visualization of seasonal shifts of phosphorus re-translocation and overwintering recycling in a shortened annual cycle system of the deciduous poplar tree (*Populus alba* L.).

Authors / Affiliations

Yuko Kurita[1,2], Satomi Kanno[1,3], Ryohei Sugita[4], Atsushi Hirose[4], Miwa Ohnishi[1], Kimitsune Ishizaki[1], Hidehiro Fukaki[1], Keitaro Tanoi[4,5], Tomoko M. Nakanishi[4], Kei'ichi Baba[6], Tetsuro Mimura[1]

[1] Department of Biology, Graduate School of Science, Kobe University, Rokkodai, Nada, Kobe, 657-8501 Japan.

[2] Faculty of Agriculture, Ryukoku University, 1-5 Yokotani, Ooe-cho, Seta, Otsu, Shiga 520-2194 Japan

[3] The French Alternative Energies and Atomic Energy Commission, France

[4] Graduate School of Agricultural and Life Sciences, The University of Tokyo, 1-1-1,Yayoi, Bunkyo-ku, Tokyo, 113-8657 Japan.

[5] JST PRESTO,

[6] Research Institute for Sustainable Humanosphere, Kyoto University, Gokasho, Uji, Kyoto, 611-0011 Japan.

Author for correspondence: Tetsuro Mimura

Tel: +81-(0)78-803-5708

e-mail: mimura@kobe-u.ac.jp

Total word count for the main body	4595 words
Introduction	717 words
Materials and Methods	1586 words
Results	914 words
Discussion	1378 words

The number of figures (in color)	6 (6)
The number of supporting information	8

Summary

(1) the research conducted, including the rationale

・ Phosphorus (P) is an essential macronutrient for plant growth. In deciduous trees, P is remobilized from senescing leaves and stored in perennial tissues during winter for further growth. To clarify how deciduous trees utilize the internal P through a year, seasonal re-translocation routes and the reuse of P over winter were investigated.

(2) methods

・ We analyzed the seasonal re-translocation and accumulation of P in poplar trees (*Populus alba*. L) cultivated under "a shortened annual cycle system", which mimicked seasonal phenology in a laboratory. The real-time radioisotope imaging and the macro- and micro-autoradiography with ^{32}P and ^{33}P were used to reveal the organ and tissue level P allocation.

(3) key results

・ The direction of phosphate re-translocation changed seasonally. In the growing season, P was mainly re-translocated from a leaf to upper parts via phloem. During senescence, P was re-translocated to lower perennial parts, and also to inner xylem parenchyma cells. Phloem-xylem exchange of re-translocated P occurred in the stem. After bud burst in spring, stored P was re-translocated to the whole plant and mainly accumulated in new shoots.

(4) the main conclusion, including the key points of discussion

・ Poplar trees change the routes of P re-translocation longitudinally and radially depending on the season, and recycle internal P throughout the year.

Key words

Autoradiography・Deciduous tree・Phosphorus・*Populus alba*・Seasonal re-translocation

Introduction

Phosphorus (P) is an essential macronutrient for plant growth, but its availability in soil is quite limited (Schachtman *et al.*, 1998). To utilize the precious P, plants have various strategies for the uptake, translocation, storage and recycling of P, etc. Re-translocation of P is a strategy for its internal recycling *in planta*. P is re-translocated from source tissues (e.g. old leaves) to sink tissues (e.g. young leaves, shoot apex) as phosphate (Biddulph *et al.*, 1958b; Mimura *et al.*, 1996; Himelblau & Amasino, 2001). It is supposed that such re-translocation of phosphate between tissues occurs via the phloem. Both downward and upward P re-translocation via the phloem from leaves, and the lateral movement from the phloem to xylem have been demonstrated using microradiographic methods in an herbaceous plant, red kidney bean (Biddulph, 1956; Biddulph *et al.*, 1958a).

In deciduous woody plants, the internal recycling of various nutrients has been studied using radiolabeled materials. Carbon (C) and sulfur (S) were shown to be re-translocated from leaves in a leaf age-dependent manner in cottonwood and *Populus tremula* × *P. alba,* respectively (Dickson, 1989; Hartmann *et al.*, 2000). These studies showed that expanding leaves daily re-translocate the remobilized nutrients mainly into source organs in the upper apical parts of the tree. On the other hand, old mature leaves re-translocated the nutrients mainly into lower parts of the tree (lower stem and roots). Dickson (1989) concluded that C transport from source leaves to sink tissues is controlled by both the vascular connections and relative sink demand.

Besides this daily re-translocation of nutrients, deciduous woody plants seasonally remobilize various nutrients including phosphorus from senescing leaves to perennial tissues during autumn, by rescuing these precious nutrients before the leaves

86 fall (Chapin & Kedrowski, 1983; Aerts, 1996; Keskitalo *et al.*, 2005; Netzer *et al.*,
87 2017b,a).

88 Recently we found that in *Populus alba*, P is remobilized from leaves during
89 autumn senescence, and stored in perennial tissues such as twigs during winter as phytic
90 acid (myo-inositol-1,2,3,4,5,6-hexakis phosphate: IP_6) (Kurita *et al.*, 2014, 2017). It is
91 well-known that phytic acid is a major P-storage form in seeds (Raboy *et al.*, 2001).
92 Kurita et al. (2014, 2017) showed that at the beginning of spring, IP_6 levels in twigs
93 decreased, presumably to release P for new growth.

94 Although the seasonal distribution of P is becoming clearer, there is little
95 information on how P is seasonally re-distributed in woody plants. For example, perennial
96 tissues like twigs function as both sink and source. Twigs are not expected to be main
97 sinks during the developmental season, although cambium zones must have sink ability
98 for their secondary growth. However, during senescence, their sink ability increases as
99 they begin to store nutrients for winter. In early spring, the twigs probably revert to
100 become source tissues, and release the stored nutrients for new growing tissues.

101 In the stems of woody plants, cells form three-dimensional lattices and they
102 transport water and solute along both the longitudinal axis and radial axes (Van Bel,
103 1990; Spicer, 2014). It is expected that the P re-translocation route also shifts dependent
104 on the seasons. However, seasonal P re-translocation routes and mechanisms, and the
105 contribution of phloem and xylem for it are currently unknown (Rennenberg &
106 Herschbach, 2013).

107 It is quite difficult and very time-consuming to investigate the detailed
108 mechanisms of nutrient re-translocation using trees grown outdoors in the field. Recently,
109 we have developed a shortened annual cycle system to facilitate the investigation of the

110 seasonal phenology in the laboratory (Kurita *et al.*, 2014). This system consists of 3
111 stages. Stage 1 mimics spring/summer, stage 2 does autumn and stage 3 does winter,
112 respectively (for detail, see method and Fig. S1c). After leaf fall in Stage 3, plants were
113 transferred to stage 1 again and bud burst induced. In this system, poplar trees showed
114 normal seasonal events (leaf coloration, leaf fall, bud burst) and seasonal P recycling
115 events (e.g. the P remobilization from senescing leaves, the storing of IP_6 in dormant
116 stems and the redistribution during budburst) (Kurita *et al.*, 2017).
117 In the present study, in order to clarify the pathways involved in phosphate re-
118 translocation and its accumulation, we used this shortened annual cycle system in the
119 laboratory with radio labeled phosphates. We succeeded in visualizing the
120 spatiotemporally diverse P re-translocation using several autoradiography methods which
121 cannot be applied to the field-grown plants.
122

Materials and Methods

Plant materials and culture conditions

Poplar shoots with 4-5 leaves were cut and rooted in 1/5 MS medium, and transferred into the pots containing vermiculite, that had been washed with tap water ten times and by distilled water five times. Potted cuttings were placed in tree culture chambers (LH-350S, NK system, Osaka, Japan) in turn from stage 1 to 3 under the conditions in "a shortened annual cycle system" as described before (Kurita *et al.*, 2014)(Fig. S1c). Briefly, stage 1 (25℃, 14h light) mimics spring/summer condition, and promotes vigorous plant growth. Stage 2 (15℃, 8h light) mimics autumn condition, and causes plants to experience short daylength and moderate cooler temperatures. Stage 3 (5℃, 8h light) mimics winter condition, and promotes leaf senescence. At this stage, plants cease apical growth. The leaves turn yellow and then fall.

Plants were fertilized with 1/5 MS medium (1L / 6 potted cuttings) once a week at stage 1. Afterwards they were cultured with distilled water only. In stages 1 and 2, plants at 3rd to 4th week, and in stage 3, plants at 3rd to 5th week, were used for the experiments.

Imaging using the real-time radioisotope imaging system

To add radiophosphorus, a "flap" was cut along a vein of 6th leaf in the manner shown in Fig.S1a (Biddulph & Markle, 1944), and 5 µl ^{32}P-phospate ($H_3{}^{32}PO_4$) solution in 0.2M KH_2PO_4 (final concentration of 200 kBq µl^{-1}) was added. After 1 or 3 min, the flap was cut off because its strong signals disturb the imaging. Then, changes in ^{32}P distribution were observed using a real-time radioisotope imaging system (RRIS) established previously (Kanno *et al.*, 2012; Hirose *et al.*, 2013; Sugita *et al.*, 2013; Sugita *et al.*, 2016). The plant

147 was mounted on the fiber optic plate coated with 100 μm thickness of CsI (Tl) scintillator
148 by vapor deposition (FOS, 100 mm × 100 mm × 5 mm, Hamamatsu Photonics Co.,
149 Hamamatsu, Japan). Two fiber optic plates were connected longitudinally. The beta ray
150 emitted from ^{32}P in the sample interacts with the CsI (Tl) scintillator, and then is converted
151 to visual light. Light was captured by the cooled CCD camera
152 (AQUACOSMOS/VIMsystem, 640 × 480 pixel; Hamamatsu Photonics, Co, Hamamatsu
153 City, Japan) with an image capture system (Aquacosmos/VIM system; resolution: 640 pixel
154 × 480 pixel, Hamamatsu Photonics Co.) (Kanno *et al.*, 2012; Sugita *et al.*, 2013). The
155 measurement was performed for three hours in a dark room at 20°C. The same
156 measurements were repeated 3 times.

157 To analyze the velocity of ^{32}P transported in the vascular bundle, the signal
158 intensity of the region of interest (ROI) was measured by ImageJ software. Two ROIs were
159 set at the apex and the 6th leaf axil. Three ROIs were set at corners of FOS to measure
160 background signals. Of the 3 replicates, the 2 trees which showed the highest signals were
161 analyzed. The velocity was calculated from the distance between the apex and the 6th leaf
162 axil and the difference between the times it took for the signal to reach the detection
163 threshold. The detection threshold was defined as five times the standard deviation of the
164 background signal intensity.

165

166 **Whole plant autoradiography using imaging plate**

167 ^{32}P-phospate (5 μl) in 0.2M KH_2PO_4 (final concentration of 200 Bq μl^{-1}) was added
168 to 6th leaf as described above. Then, plants were cultured in each stage condition for 1 day.
169 After 1 day culture, the 6th leaf was cut off because its strong signals disturb the imaging.
170 The vermiculite was washed away from poplar roots with tap water. Plants were then

171 mounted on commercial xerographic paper, and wrapped with double layers of polyvinyl
172 film. The sample was set on the imaging plate (Fujifilm, Tokyo, Japan) in the cassette case
173 and exposed in a dark room for 3 days. The imaging plate was then measured using
174 Typhoon FLA 9500 (GE Healthcare UK Ltd., Buckinghamshire, England). The same
175 measurements were repeated 3 times.
176
177 **Whole plant autoradiography using imaging plate with phloem girdling**
178 Approximately 2 mm of bark from the upper or lower internodes of the 6th leaf of a
179 plant at stage 1 was cut with a razor blade and peeled off, effectively disrupting phloem
180 translocation in this region (Fig. S1b). Then immediately, 5 μl ^{32}P-phospate ($KH_2{}^{32}PO_4$)
181 solution in 0.2 M KH_2PO_4 (final concentration of 1 kBq μl^{-1}) was added to the 6th leaf as
182 described above. Plants were cultured in stage 1 for 3 h or 1 day. After culture, the 6th leaf
183 was cut off. Upper and lower internodes of 6th leaf were cut to prevent re-translocation of
184 ^{32}P during contact. The vermiculite was washed away from poplar roots with tap water.
185 Plants were then mounted on commercial xerographic paper and wrapped with double
186 layers of polyvinyl film. The sample was set on the imaging plate in the cassette case and
187 exposed in a dark room for 1 day. Then the imaging plate was measured using Typhoon
188 FLA 9500. The same measurements were repeated 3 times.
189
190 **Microautoradiography (MAR) of the stem**
191 ^{33}P-phospate (5 μl) in 0.2M KH_2PO_4 (final concentration of 37 or 74 kBq μl^{-1}) was
192 added to 6th leaf as described above. Then, plants were cultured in each stage condition for
193 1 day. ^{32}P is not suitable for obtaining high-resolution images because its energy is too high.
194 Therefore, the experiments were performed by using ^{33}P which has a lower energy. ^{33}P

195 distribution in stems was detected by the MAR method for fresh-frozen sections, as
196 described previously (Hirose *et al.*, 2014). Stem samples that were cut from a poplar in
197 each stage, were frozen with liquid nitrogen. The frozen stems were embedded in a
198 dedicated embedding medium (SCEM; SECTION-LAB Co. Ltd.) and sliced into 20 μm
199 thick sections using a Cryostat (CM1850; Leica Microsystems, Wetzlar, Germany) set at
200 −20°C. Sectioning was performed using the Cryo-Film transfer kit (SECTION-LAB Co.
201 Ltd., Hiroshima, Japan) (Kawamoto, 2003; Hirose *et al.*, 2014).

202 Frozen sections were put on hydrophilic amino-coated glass slides (MAS-GP type A;
203 Matsunami Glass Ind., Ltd., Osaka, Japan) coated with a photosensitive nuclear emulsion
204 (Ilford Nuclear Emulsion Type K5; Harman Technology Ltd., Cheshire, UK) in the
205 Cryostat, and contacted tightly at −80°C for approximately 1 month or more. A 1.2 μm
206 thick polyphenylene sulfide (PPS) film was inserted between the frozen sample sections
207 and the photosensitive nuclear emulsion on the glass slide to enable easy separation of the
208 section and the emulsion after exposure. The results scarcely changed when the sample was
209 exposed for more than 1 month.

210 After the exposure, the sections were removed from the glass slides in the cryostat set
211 at −20°C in the darkroom. The glass slides were soaked in quarter-strength D-19 developer
212 (Eastman Kodak Co., NY, USA) for 6 min at room temperature to develop the silver
213 particles. Then, the slides were soaked in distilled water for 1 min to stop the development,
214 followed by exposure to 0.83 M sodium thiosulfate for 4 min for fixation. Finally, the glass
215 slides were soaked in distilled water for 10 min twice. The temperature of the darkroom
216 was maintained at 20°C to ensure development.

217 In order to stain the sliced tissue, the sections were floated on distilled water for 1 min
218 three times at room temperature to wash out the embedding material. Then the sections

219 were stained with 0.25 % toluidine blue for 30 sec and rinsed with water for 1 min. The
220 sections were then mounted on a new glass slide using a glycerol-based mounting medium
221 (SCMM; SECTION-LAB Co. Ltd.).

222 The stained sections and the silver particles developed by MAR were observed and
223 photographed using a microscope (BX-60; Olympus, Tokyo, Japan). The tissue images and
224 radiographs were then assembled using e-Tiling (Mitani Co., Tokyo, Japan) or ImageJ
225 (http://rsb.info.nih.gov/ij) by its plugin, Grid/Collection stitching software (Preibisch *et al.*,
226 2009). The registration was performed on the tissue images and radiographs using ImageJ
227 and LPixel's ImageJ Plugin, Lpx Registration software (https://lpixel.net/products/lpixel-
228 imagej-plugins/) and GIMP software (http://www.gimp.org). The same measurements
229 were repeated 3 times.

230

231 **Autoradiography of the leaf axil and 3D construction**

232 Fresh-frozen sections from the axil of the sixth leaf were prepared for autoradiography
233 experiments using the imaging plate (BAS IP MS; GE Healthcare UK Ltd.). The thickness
234 of the section was 20 μm. The exposure time was about 76 h for samples in stage 1 at −
235 80°C. In stage 3, exposure time was about 22 h because the signal was stronger than that of
236 samples in stage 1. The imaging plate was scanned with an FLA5000 image analyser
237 (Fujifilm, Tokyo, Japan) at a resolution of 10 μm.

238 After linear contrast enhancement and registration using ImageJ pluguin StackReg
239 (Thévenaz *et al.*, 1998), autoradiographs were converted to 3D images using ImageJ plugin
240 Volume Viewer (http://rsb.info.nih.gov/ij/plugins/volume-viewer.html) and 3D Viewer
241 (http://imagej.nih.gov/ij/plugins/3d-viewer/). The same measurements were repeated 3
242 times.

243

244 **Whole plant autoradiography using imaging plate over dormancy period**

245 ^{32}P-phospate (7 μl) in 0.2M KH_2PO_4 (final concentration of 700k Bq μl^{-1}) was added
246 to 6th leaf of a plant at 4th week in stage 3 as described above. After leaf fall (at 8th week
247 in stage 3) or after bud burst (at 2nd week in stage 1 of 2nd cycle), the vermiculite was
248 washed away from poplar roots with tap water. The plant was then mounted on paper, and
249 wrapped with a double layer of polyvinyl film. The sample was set on the imaging plate
250 in the cassette case and exposed in a dark room for 15min or 1 day. Then, the imaging
251 plate was measured using Typhoon FLA 9500. The same measurements were repeated 3
252 times.

253

Results

Shift of longitudinal re-translocation routes of phosphorus between growing and senescence seasons.

To continuously observe how P is re-translocated from a leaf, we performed real-time radioisotope imaging using plants grown in the shortened annual cycle system. In stage 1, ^{32}P was re-translocated from the 6th leaf in both upward and downward directions, and gradually accumulated at apical parts (apex and young leaves) in 3h (Fig.1a, Video S1, Fig. S2). Within 30 min, ^{32}P was detected at the leaf axil of the applied leaves, and after 1 to 1.5 h, ^{32}P was detected at the shoot apex. Estimated transport velocities were about 0.015 mm s^{-1} in tree A and 0.021 mm s^{-1} in tree B (Fig. S2). On the other hand, in stage 3, ^{32}P was only re-translocated downwards from the 6th leaf. No signals in upper parts were detected within 3h (Fig.1b, Video S2). To observe ^{32}P transport and distribution in whole plants over longer periods, plants were cultured for 1 day after ^{32}P application, and contacted to imaging plates (Fig.2). In stage 1, ^{32}P was detected mainly in the upper parts, in agreement with the results of the real-time imaging experiment. During stages 2 and 3, ^{32}P was detected mainly in the lower parts (stem and roots), and slightly in the upper stem.

Longitudinal re-translocation of phosphorus via phloem.

To reveal which tissue (xylem and/or phloem) is involved in longitudinal re-translocation of P, changes in the re-translocation route of P were observed by phloem girdling using a tree in stage 1 (Fig. 3, S1b). The upper or lower phloem of a node attached to the 6th leaf was peeled off, and then ^{32}P was immediately applied to the 6th leaf. After 3 h or 1 day culture, the plant was set on imaging plate for ^{32}P detection. When the phloem was peeled off above the applied leaf, ^{32}P was detected only in the lower stem and roots

279 after 3 h (Fig.3a). After 1 day, ^{32}P was detected mainly in the lower stem and roots, and
280 slightly in the upper stem and young leaves. When phloem was peeled off below the applied
281 leaf, ^{32}P was detected only in the upper stem and young leaves after 3 h or 1 day culture
282 (Fig.3b).
283
284 **Visualization of P inflow from a leaf to the stem**
285 To observe P inflow from a leaf to the stem in detail, serial autoradiographs of a
286 leaf axil were converted to 3D images (Fig. 4a, b and S3). ^{33}P was used for more detailed
287 observation in these experiments. In each stage, plants were cultured for 1 day after ^{33}P
288 application. In stage 1, ^{33}P was detected throughout the stem, petiole and bud. In the stem,
289 ^{33}P was mainly distributed in the phloem region on the side of applied leaf (Fig. 4a, S3a,
290 Video S3). On the other hand, in stage 3, ^{33}P wad strongly detected in the lower phloem on
291 the applied side of the leaf and petiole (Fig. 4b, S3b, Video S4). ^{33}P was barely detected in
292 the upper stem, axillary bud or the phloem opposite the petiole. At the junction between the
293 petiole and the stem, there appeared to be formation of an abscission layer (Fig. 4b, S3b).
294
295 **Shift of radial P re-translocation from a leaf between growing and senescence seasons.**
296 To observe radial transport inside a stem during senescence, we used
297 microautoradiography because of its higher resolution compared to conventional
298 autoradiography using an imaging plate. Plants on which ^{33}P was applied to the 6th leaf
299 were cultured for one day. ^{33}P localization in fresh frozen sections of the stem was detected.
300 In the growing season at stage 1, ^{33}P was detected mainly in phloem and to a lesser extent
301 throughout the section of the stem just below the 6th leaf (stem between 6th and 7th nodes)
302 (Fig. 4c). As shown in the 3D reconstruction (Fig. 4a), the highest signals were recorded in

303 the phloem on the side of the ^{33}P applied leaf. This tendency was also observed in the upper
304 stem (stem between 5th and 6th nodes) and the lower stem (stem between 9th and 10th nodes)
305 (Fig. S4a, b).

306 During senescence at stage 3, ^{33}P was strongly detected in the phloem on the side
307 of the applied leaf, and also in ray tissues and parenchyma cells around the pith
308 (perimedullary cells) (Fig. 4d). ^{33}P was slightly detected both in the upper stem (stem
309 between 5th and 6th nodes) and the lower stem (stem between 9th and 10th nodes) (Fig. S4c,
310 d). Because ^{33}P accumulation was stronger in the stem between 6th and 7th nodes than in the
311 stem between 9th and 10th nodes, the exchange from phloem to xylem probably occurred in
312 the stem nearby the applied leaf rather than in the lower stem and roots.

313

314 **Re-utilization of overwintering P stored in stem and roots by new growing tissues in**
315 **spring.**

316 To reveal how P stored in winter is re-utilized in spring, artificial overwinter
317 experiments were performed in the shortened annual cycle system (Fig. 5). Plants, which
318 had ^{32}P applied to the 6th leaf were cultured for about 1 month until leaf fall in stage 3. Just
319 after leaf fall, ^{32}P was detected mainly in the lower stem and roots (Fig. 5a). Other trees
320 were moved to stage 1 and bud burst induced. After bud burst in plants put in the second
321 shortened annual cycle, ^{32}P remobilized from the 6th leaf was detected throughout the whole
322 plant, particularly at apices and young leaves of new shoots (Fig. 5b).

323

Discussion

Experimental system

Seasonal changes in re-translocation of phosphorus (P) have been investigated by measurement of phosphate contents in organs (Chapin & Kedrowski, 1983; Keskitalo *et al.*, 2005; Kurita *et al.*, 2014, 2017; Netzer *et al.*, 2017a,b).

In this study, we have attempted to realize how such P is re-translocated between organs. Our shortened annual cycle system succeeded in reproducing the annual phenology of poplar trees in a laboratory (Kurita *et al.*, 2014, 2017), and here we have used this system to visualize the seasonal changes of P re-translocation in poplar trees using radiolabeled phosphate at both whole plant level and tissue level (Fig. 6).

Seasonal shifts of P re-translocation routes from a leaf.

At stage 1, P was re-translocated from the 6th leaf mainly to younger leaves and the shoot apex (Fig. 1a, 2). These results correspond with previous studies on re-translocation of C and S from leaves (Dickson, 1989; Hartmann *et al.*, 2000). On the other hand, in stage 3, although the applied leaf position (6th) was the same, P was mainly re-translocated to the lower stem (Fig.1b, 2). This seasonal difference was more obvious in 3D images (Fig. 4). The upward transport clearly ceased at stage 3 compared with stage 1. P re-translocation to the axillary bud also changed between stage 1 and stage 3 (Fig. 4a, b). These results indicated that seasonal shifts of sink tissues and of longitudinal re-translocation routes occur between the growing season (stage 1) and senescence (stage 3). In stage 1, the apical meristem is active and trees keep growing. Then, during stages 2 to 3, trees cease apical growth and leaves start to senesce. Loss of sink ability in the apex,

348 younger leaves and axillary buds may lead to the seasonal transition of re-translocation
349 routes. In the northern red oak, it was observed that the C allocation pattern changed with
350 the timing of flushing of new leaves (Dickson, 1989).
351
352 **Real-time observation of P re-translocation from a leaf**
353 Real-time imaging revealed a rapid flow of phosphate in poplar plants (Fig. 1).
354 In stage 1, ^{32}P was re-translocated from the 6th leaf both downward and upward, and ^{32}P
355 signals were detected at the apex within 1 to 2 h (Fig.1a, S2). This rapid P re-translocation
356 probably occurred via phloem because early P re-translocation was suppressed by phloem
357 girdling (Fig. 3). The mechanism of phloem transport is generally explained by the
358 Münch Theory as mass flow driven by an osmotically generated pressure gradient
359 (Münch, 1930; De Schepper *et al.*, 2013). Windt et al. (2006) measured velocities of the
360 downward phloem flow in poplar using NMR imaging, and recorded a velocity of 0.34 ±
361 0.03 mm s^{-1} in the daytime (Windt *et al.*, 2006). Schepper et al. (2013) found that phloem
362 speed in angiosperms is roughly within the same range, around 0.17 mm s^{-1} (De Schepper
363 *et al.*, 2013). By the detection of ^{32}P signals, we estimated that the transport velocity was
364 about 0.015 mm s^{-1} to 0.021 mm s^{-1} (Fig. S2). It should be noted that this value, which is
365 considerably slower than previously reported, may probably show under-estimation. This
366 result was partly expected because the thickness of poplar stems and leaves prevent
367 instant detection of ^{32}P in the present system. In poplar stems, ^{32}P was localized in
368 internal tissues (primarily the phloem), therefore its detection might be hindered in
369 inverse proportion to the thickness of the outer tissues. It is believed that this decrease in
370 signal intensity caused the signal to fall below the detection limit, leading to detection

371 delays. Therefore, at this time, we can only discuss the direction of P transport and the
372 tissues that play a role of P re-translocation.
373
374 **Phloem-xylem exchange of P in stem.**
375 In the growing season, P re-translocated from leaves was exchanged from phloem to
376 xylem in the stem, and transported to apical parts via xylem over longer periods (Fig. 3).
377 Microautoradiography also showed the presence of re-translocated ^{33}P in both phloem
378 and xylem (Fig. 4c). Such circulation using both phloem and xylem to transport nutrients
379 coincides with previous reports in herbaceous plants (Biddulph *et al.*, 1958b) or reports
380 about other nutrients in woody plants (Hartmann *et al.*, 2000; Herschbach *et al.*, 2012).
381 However, it is unclear how P is re-translocated from phloem to xylem. Pfautsch *et al.*
382 (2015) demonstrated the radial flow of water from phloem into xylem in *Eucalyptus*
383 *saligna* by injection of a fluorescent dye. The radial transfer of water occurs
384 predominantly via the symplast of ray parenchyma cells. Radial P transport may also
385 occur symplastically along with the water flow. Although P re-translocation occurred
386 predominantly via phloem, phloem-xylem exchange would be an advantage especially for
387 long-distance transport in a tall tree. Because the xylem flow velocity (1.60 ± 0.09 mm s^{-}
388 ^{1}) is much faster than the phloem flow (Windt *et al.*, 2006), remobilized nutrients can be
389 transported to upper parts in a shorter period.
390
391 **P re-translocation and winter storage in stem.**
392 During the growth season, poplar trees re-translocate P from source tissues such as
393 mature leaves to the growing sink tissues via phloem and xylem. The stem cambium may

394 also have sink ability because the stem diameter increased at stage 1 (Baba *et al.*, 2018),
395 and ^{33}P was detected in the entire section including the cambium region (Fig. 4c).
396 On the other hand, during senescence, stem and roots function as sink tissues for
397 winter P storage (Fig. 2, 5a). In stage 3, re-translocated ^{33}P was more strongly detected in
398 xylem parenchyma cells of the stem just below the 6th leaf (stem between 6th and 7th
399 nodes) than in other parts (Fig. 4d, S4c, d). Thus, the remobilized P from a leaf is thought
400 to be immediately transferred from phloem to xylem, and stored in ray cells and
401 perimedullary cells (Fig. 6). Phloem parenchyma cells also play a role in winter storage.
402 We have previously reported that winter P is stored as IP_6 in the globoid-like structures in
403 protein storage vacuoles at phloem and xylem parenchyma cells in poplar twigs (Kurita *et*
404 *al.*, 2017). ^{33}P localization using microautoradiography (Fig. 4d) agreed with the
405 localization of globoid-like structures. Netzer *et al*. (2017a) also reported P accumulation
406 in the cambial zone and wood ray parenchyma cells of *Populus* × *canescens* during
407 dormancy.
408
409 **Re-allocation of P from the stem to new shoots in spring**
410 After bud burst, stored P was re-allocated to the whole plant, and strongly detected
411 in young leaves and the shoot apex (Fig. 5). This indicates that poplar stem and roots are
412 seasonally reversible sinks, that function as a source of P during early spring. We
413 succeeded in demonstrating that P remobilized from leaves is recycled beyond winter for
414 spring growth in *Populus alba*. Interestingly, we supplied ^{32}P to only a single 6th leaf
415 before winter, but in spring, ^{32}P was re-allocated to the whole plant from the stored parts.
416 This means that P which is stored from a leaf in winter, is re-allocated to the whole plant
417 and mixed with P from other source tissues in spring.
418

419 **Conclusion**

420 Seasonal P recycling is thought to be an adaptive strategy tailored to the lifestyle of
421 deciduous plants. In this paper, we visualized how P is seasonally re-translocated in
422 juvenile poplar trees, and clearly showed that re-translocated P from leaves was reused for
423 spring growth after overwintering.

424 The next step is to try to discover how deciduous trees regulate such seasonal P re-
425 translocation depending on environmental cues and/or internal P status. The seasonal
426 cycle of growth and dormancy, and the molecular mechanisms by which day length and
427 temperature signals regulate the annual cycle have been well studied in Populus (Maurya
428 & Bhalerao, 2017). Identification of phosphate transporters and expression profiles
429 according to tissues and P availabilities have also been reported (Loth-Pereda *et al.*, 2011;
430 Kavka & Polle, 2016). In herbaceous plants, local and systemic signaling for Pi starvation
431 is becoming increasingly understood (Chien *et al.*, 2018).

432 Although investigations of seasonal phenomena in trees take longer, the shortened
433 annual cycle system enables us to accelerate it, and to perform seasonal experiments
434 using transgenic trees more easily. The combination of laboratory and field studies will be
435 important in the elucidation of this re-translocation mechanism in mature tall trees in the
436 field, and will contribute to our understanding of the annual nutritional balance of the
437 entire tree.

Acknowledgement

We would like to offer our heartfelt thanks to Prof. Rob Reid (University of Adelaide, Australia) for his kind discussion and correction of this manuscript. We also greatly appreciate Dr. Tatsuaki Goh and Dr. Koichi Toyokura for their kind discussion and incisive comments. This work was supported by a Grant-in-Aid for Scientific Research of Innovative Areas from the Japanese Ministry of Education, Sports, Culture, Science, and Technology on ‘‘Perceptive plants (22120006)’’ and “Plant-structure-opt (18H05493)”, and JSPS KAKENHI grant Number 15J03992 and 18K14735. Y. Kurita is deeply grateful to the SUNBOR Scholarship. The authors declare no competing financial interests.

Author Contribution

YK and TM designed the study and wrote the manuscript. SK and RS instructed experiments using RRIS, and YK performed it with SK and RS. AH instructed experiments using MAR, and YK performed it with AH. KT and TMN advised experimental design using RRIS and MAR. KB instructed on dendrology. MO, HF and KI supported YK's experiments in Kobe university. All authors discussed the results and advised on the manuscript.

455 **References**

456

457 **Aerts R**. **1996**. Nutrient resorption from senescing leaves of perennials: are there general
458 patterns? *Journal of Ecology* **84**: 597–608.

459 **Baba K, Kurita Y, Mimura T**. **2018**. Wood structure of *Populus alba* formed in a
460 shortened annual cycle system. *Journal of Wood Science* **64**: 1–5.

461 **Van Bel AJE**. **1990**. Xylem-phloem exchange via the rays: The undervalued route of
462 transport. *Journal of Experimental Botany* **41**: 631–644.

463 **Biddulph SF**. **1956**. Visual indication of S^{35} and P^{32} translocation in the phloem.
464 *American Journal of Botany* **43**: 143–148.

465 **Biddulph S, Biddulph O, Cory R**. **1958a**. Visual indications of upward movement of
466 foliar-applied P^{32} and C^{14} in the phloem of the bean stem. *American Journal of Botany*
467 **45**: 648–652.

468 **Biddulph O, Biddulph S, Cory R, Koontz H**. **1958b**. Circulation patterns for
469 phosphorus, sulfur and calcium in the bean plant. *Plant Physiology* **33**: 293–300.

470 **Biddulph O, Markle J**. **1944**. Translocation of radiophosphorus in the phloem of the
471 cotton plant. *American Journal of Botany* **31**: 65–70.

472 **Chapin FS, Kedrowski RA**. **1983**. Seasonal changes in nitrogen and phosphorus
473 fractions and autumn retranslocation in evergreen and deciduous taiga trees. *Ecology* **64**:
474 376–391.

475 **Chien PS, Chiang CP, Leong SJ, Chiou TJ**. **2018**. Sensing and Signaling of Phosphate
476 Starvation: From Local to Long Distance. *Plant and Cell Physiology* **59**: 1714–1722.

477 **Dickson RE**. **1989**. Carbon and nitrogen allocation in trees. *Transport* **46**: 631s-647s.

478 **Hartmann T, Mult S, Suter M, Rennenberg H, Herschbach C**. **2000**. Leaf age-

479 dependent differences in sulphur assimilation and allocation in poplar (*Populus tremula* x
480 *P. alba*) leaves. *Journal of Experimental Botany* **51**: 1077–1088.
481 **Herschbach C, Gessler A, Rennenberg H**. **2012**. Long-distance transport and plant
482 internal cycling of N- and S-compounds. *Progress in Botany* **73**: 161–188.
483 **Himelblau E, Amasino RM**. **2001**. Nutrients mobilized from leaves of *Arabidopsis*
484 *thaliana* during leaf senescence. *Journal of Plant Physiology* **158**: 1317–1323.
485 **Hirose A, Kobayashi NI, Tanoi K, Nakanishi TM**. **2014**. A Microautoradiographic
486 Method for Fresh-Frozen Sections to Reveal the Distribution of Radionuclides at the
487 Cellular Level in Plants. *Plant and Cell Physiology* **55**: 1194–1202.
488 **Hirose A, Yamawaki M, Kanno S, Igarashi S, Sugita R, Ohmae Y, Tanoi K,**
489 **Nakanishi TM**. **2013**. Development of a ^{14}C detectable real-time radioisotope imaging
490 system for plants under intermittent light environment. *Journal of Radioanalytical and*
491 *Nuclear Chemistry* **296**: 417–422.
492 **Kanno S, Yamawaki M, Ishibashi H, Kobayashi NI, Hirose A, Tanoi K, Nussaume**
493 **L, Nakanishi TM**. **2012**. Development of real-time radioisotope imaging systems for
494 plant nutrient uptake studies. *Philosophical Transactions of the Royal Society B:*
495 *Biological Sciences* **367**: 1501–1508.
496 **Kavka M, Polle A**. **2016**. Phosphate uptake kinetics and tissue-specific transporter
497 expression profiles in poplar (*Populus* × *canescens*) at different phosphorus availabilities.
498 *BMC Plant Biology* **16**: 206.
499 **Kawamoto T**. **2003**. Use of a new adhesive film for the preparation of multi-purpose
500 fresh-frozen sections from hard tissues, whole-animals, insects and plants. *Archives of*
501 *histology and cytology* **66**: 123–143.
502 **Keskitalo J, Bergquist G, Gardenström P, Jansson S**. **2005**. A cellular timetable of

503 autumn senescence. *Plant Physiology* **139**: 1635–1648.

504 **Kurita Y, Baba K, Ohnishi M, Anegawa A, Shichijo C, Kosuge K, Fukaki H,**
505 **Mimura T**. **2014**. Establishment of a shortened annual cycle system ; a tool for the
506 analysis of annual re-translocation of phosphorus in the deciduous woody plant (*Populus*
507 *alba* L .). *Journal of Plant Research* **127**: 545–551.

508 **Kurita Y, Baba K, Ohnishi M, Matsubara R, Kosuge K, Anegawa A, Shichijo C,**
509 **Ishizaki K, Kaneko Y, Hayashi M, *et al.* 2017**. Inositol Hexakis Phosphate is the
510 Seasonal Phosphorus Reservoir in the Deciduous Woody Plant *Populus alba* L. *Plant and*
511 *Cell Physiology* **58**: 1477–1485.

512 **Loth-Pereda V, Orsini E, Courty PE, Lota F, Kohler A, Diss L, Blaudez D, Chalot**
513 **M, Nehls U, Bucher M, *et al.* 2011**. Structure and Expression Profile of the Phosphate
514 Pht1 Transporter Gene Family in Mycorrhizal Populus trichocarpa. *Plant physiology* **156**:
515 2141–2154.

516 **Maurya JP, Bhalerao RP**. **2017**. Photoperiod- and temperature-mediated control of
517 growth cessation and dormancy in trees: A molecular perspective. *Annals of Botany* **120**:
518 351–360.

519 **Mimura T, Sakano K, Shimmen T**. **1996**. Studies on the distribution, re-transiocation
520 and homeostasis of inorganic phosphate in barley leaves. *Plant, Cell and Environment* **19**:
521 311–320.

522 **Münch E**. **1930**. Die Stoffbewegung in der Pflanze. *Jena: Fischer*.

523 **Netzer F, Mueller CW, Scheerer U, Grüner J, Kögel-Knabner I, Herschbach C,**
524 **Rennenberg H**. **2017a**. Phosphorus nutrition of *Populus* × *canescens* reflects adaptation
525 to high P-availability in the soil. *Tree Physiology*: 1–19.

526 **Netzer F, Schmid C, Herschbach C, Rennenberg H**. **2017b**. Phosphorus-nutrition of

527 European beech (*Fagus sylvatica* L.) during annual growth depends on tree age and P-
528 availability in the soil. *Environmental and Experimental Botany* **137**: 194–207.
529 **Preibisch S, Saalfeld S, Tomancak P**. **2009**. Globally optimal stitching of tiled 3D
530 microscopic image acquisitions. *Bioinformatics* **25**: 1463–1465.
531 **Raboy V, Young K a, Dorsch J a, Cook A**. **2001**. Genetics and breeding of seed
532 phosphorus and phytic acid. *Journal of Plant Physiology* **158**: 489–497.
533 **Rennenberg H, Herschbach C**. **2013**. Phosphorus nutrition of woody plants: many
534 questions - few answers. *Plant Biology* **15**: 785–788.
535 **Salisbury FB, Ross CW**. **1992**. Plant physiology. In: Belmont, CA.: Wadsworth.
536 **Schachtman DP, Reid RJ, Ayling SM**. **1998**. Phosphorus uptake by plants : from soil to
537 cell. *Plant physiology* **116**: 447–453.
538 **De Schepper V, De Swaef T, Bauweraerts I, Steppe K**. **2013**. Phloem transport: A
539 review of mechanisms and controls. *Journal of Experimental Botany* **64**: 4839–4850.
540 **Spicer R**. **2014**. Symplasmic networks in secondary vascular tissues: Parenchyma
541 distribution and activity supporting long-distance transport. *Journal of Experimental*
542 *Botany* **65**: 1829–1848.
543 **Sugita R, Kobayashi NI, Hirose A, Ohmae Y, Tanoi K, Nakanishi TM**. **2013**.
544 Nondestructive real-time radioisotope imaging system for visualizing ^{14}C-labeled
545 chemicals supplied as CO_2 in plants using *Arabidopsis thaliana*. *Journal of*
546 *Radioanalytical and Nuclear Chemistry* **298**: 1411–1416.
547 **Sugita R, Kobayashi NI, Hirose A, Saito T, Iwata R, Tanoi K, Nakanishi TM. 2016.**
548 Visualization of uptake of mineral elements and the dynamics of photosynthates in
549 *Arabidopsis* by a newly developed real-time radioisotope imaging system (RRIS). *Plant*
550 *and Cell Physiology*, **57**: 743-753.

Thévenaz P, Ruttiman UE, Unser M. **1998**. A Pyramid Approach to Sub-Pixel Registraion based on Intensity. *IEEE Trans. Image Processing* **7**: 27–41.

Windt CW, Vergeldt FJ, De Jager PA, Van As H. **2006**. MRI of long-distance water transport: A comparison of the phloem and xylem flow characteristics and dynamics in poplar, castor bean, tomato and tobacco. *Plant, Cell and Environment* **29**: 1715–1729.

Figures

Fig. 1 Real-time imaging of ^{32}P in *Populus alba*. (a) At stage 1. (b) At stage 3. Pink color triangles indicate the position of 6th leaf. The 6th leaf was shielded by acrylic board because its strong signals disturb measurement. bar = 2 cm.

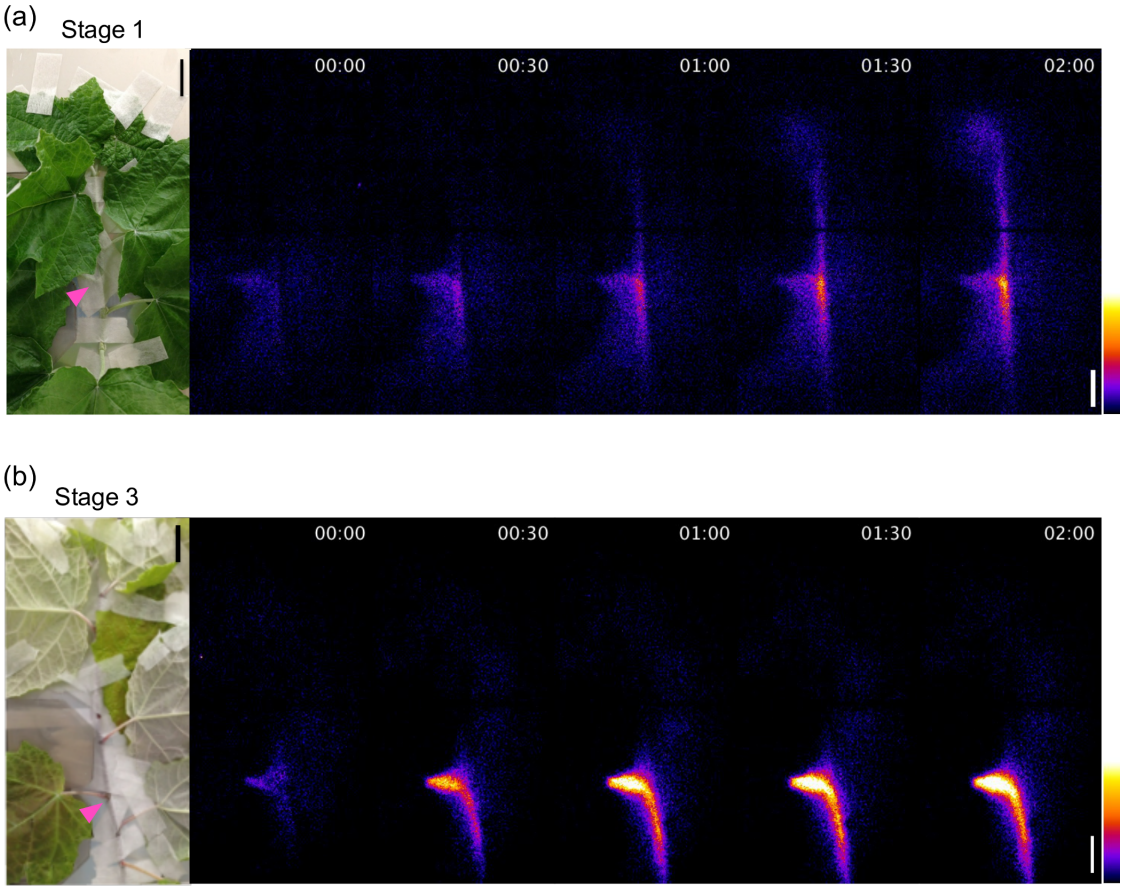

Fig. 2 Whole plant autoradiographs of *Populus alba* trees in a shortened annual cycle system. Images after one day of ^{32}P application at each stage. Pink color triangles indicate the position of 6th leaf. The 6th leaf was cut off because its strong signals disturb measurement. In stage 2 and 3, the stem was cut because the plant was too large for the imaging plate. bar = 4 cm.

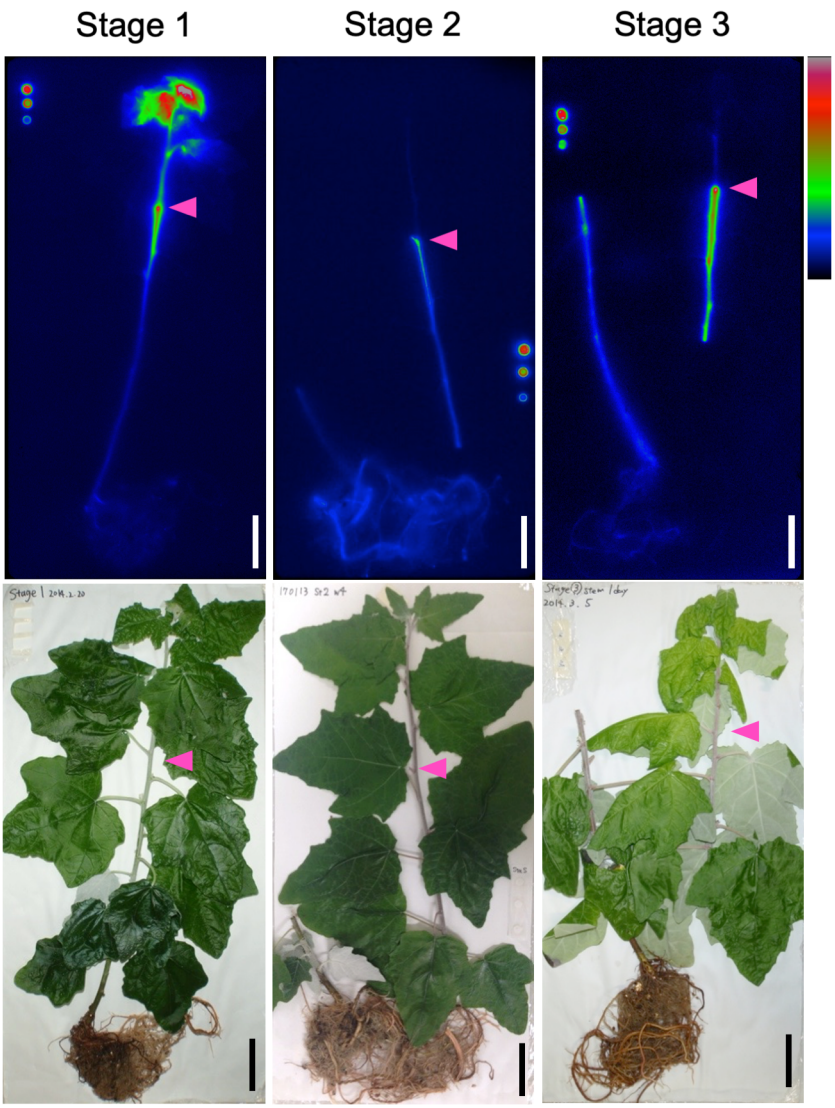

Fig. 3 Whole plant autoradiographs of *Populus alba* trees with phloem girdling. **(a)** Plants peeled of their upper bark from the 6th leaf were cultured for 3 h or 24 h. **(b)** Plants peeled of their lower bark from the 6th leaf were cultured for 3 h or 24 h. Plants at stage 1 were used for experiments. ^{32}P solution was added to the 6th leaf indicated by pink color triangles. Blue color triangles indicate the position of phloem girdling. After cultivation, upper and lower internodes of the 6th leaf were cut to prevent further re-translocation of ^{32}P during contact. bar = 4 cm.

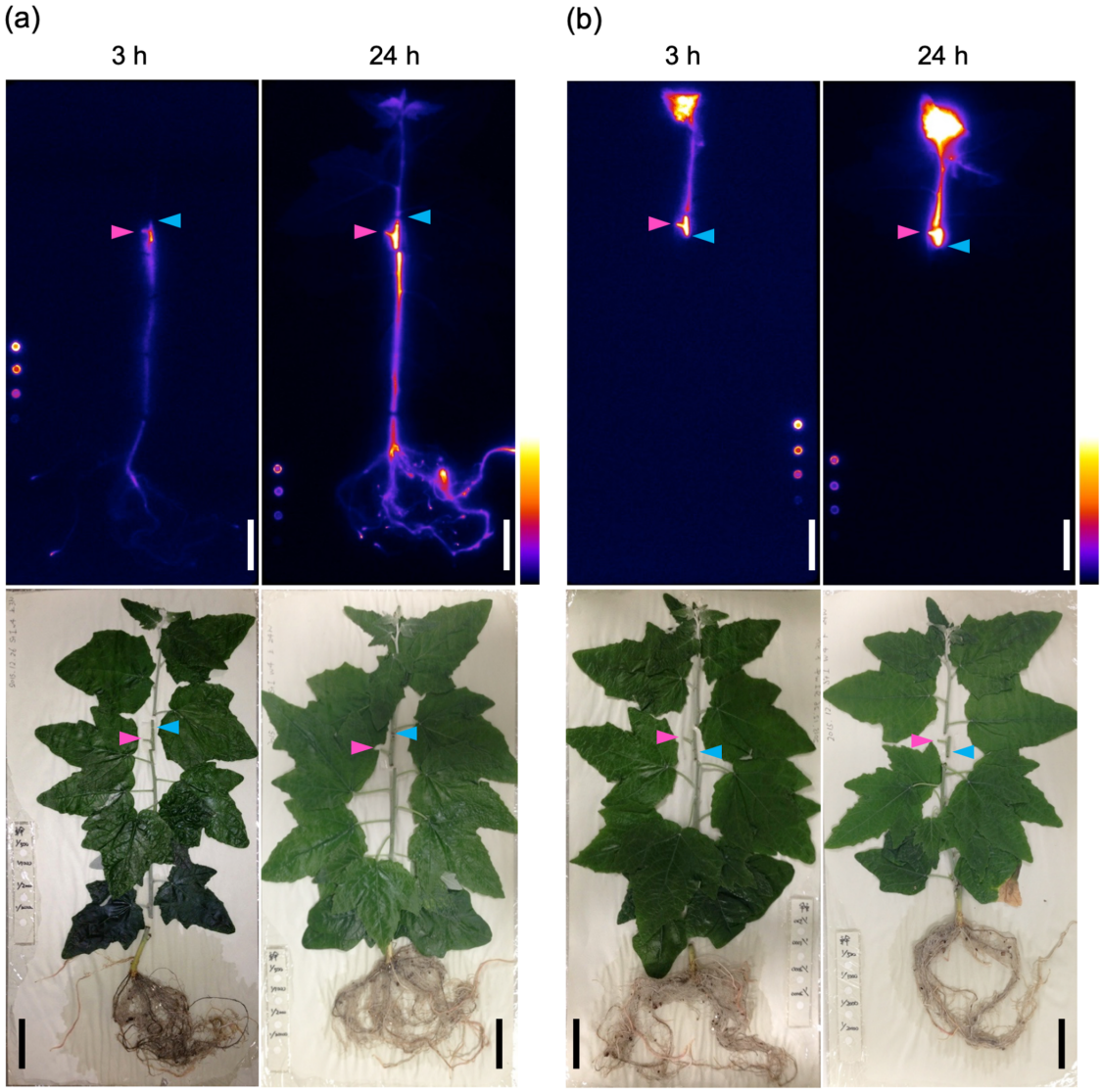

576 **Fig. 4** Side view of the 6th axil and microautoradiographs of the stem between the 6th
577 and 7th nodes of *Populus alba*. (a) Side view of the 6th axil at stage 1. ^{33}P autoradiograph
578 sections were assembled into 3D images using ImageJ. (b) Side view of the 6th axil at
579 stage 3. The white color triangle indicates abscission layer during formation. (c) The stem
580 between 6th and 7th nodes in stage 1. Left: section stained by toluidine blue. Middle:
581 microautoradiograph of the section. Right: merged image. Green color triangles indicate
582 the position of the 6th leaf. (d) The stem between 6th and 7th nodes in stage 3. Bar = 0.5
583 mm.
584
585

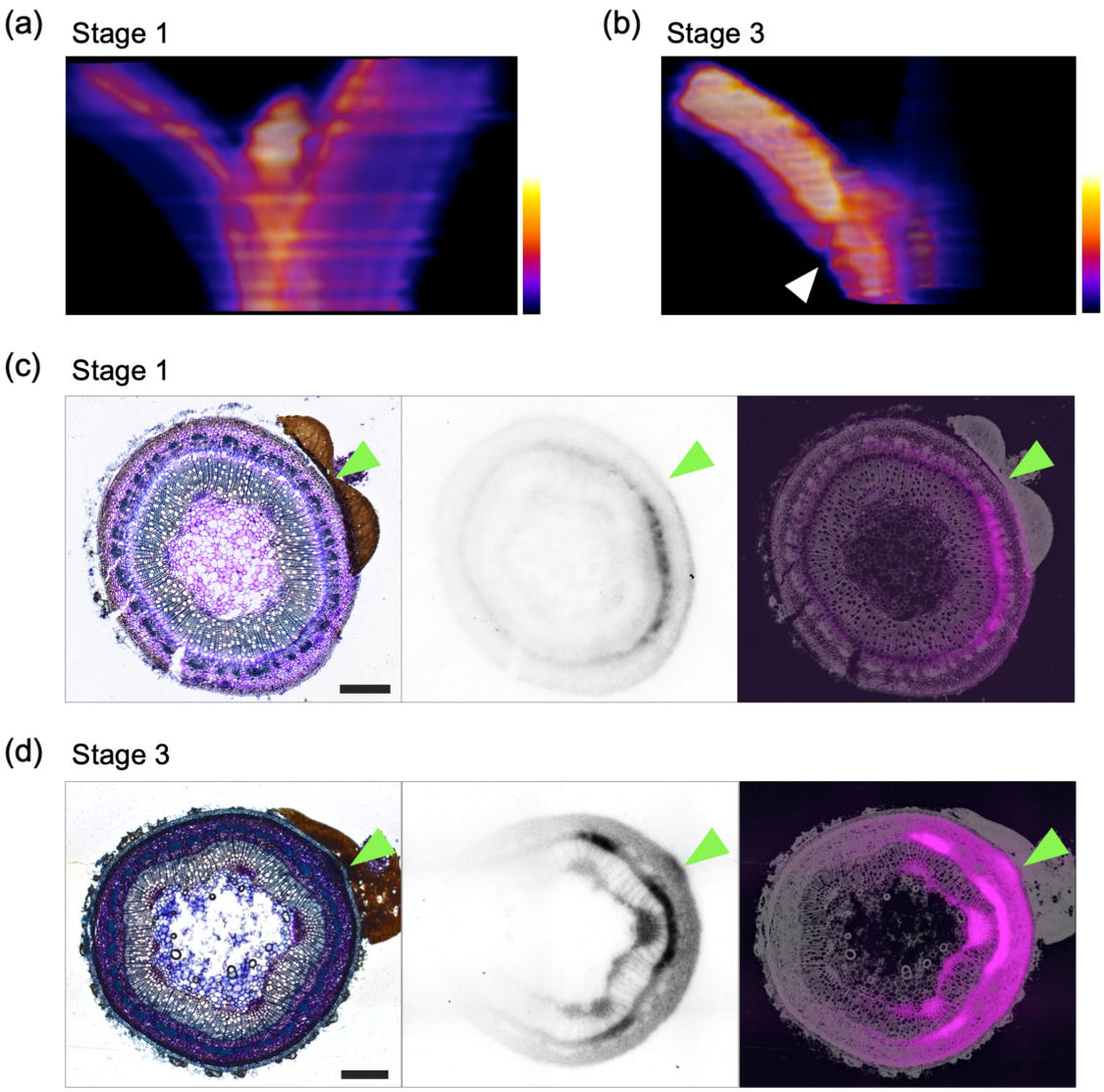

Fig. 5 Whole plant autoradiographs of *Populus alba* trees in the shortened annual cycle system. Poplar trees in which ^{32}P was applied to the 6th leaf at 4th week in stage 3 were subsequently cultured in stage 3. (a) Image after 4 weeks of ^{32}P application (just after leaf fall). (b) Image after 6 weeks of ^{32}P application. After 4 weeks cultivation, plants were moved to stage 1, and bud burst was induced. Pink color triangles indicate the position of the 6th leaf. The stem was cut because the plant was too large for the imaging plate. bar = 4 cm.

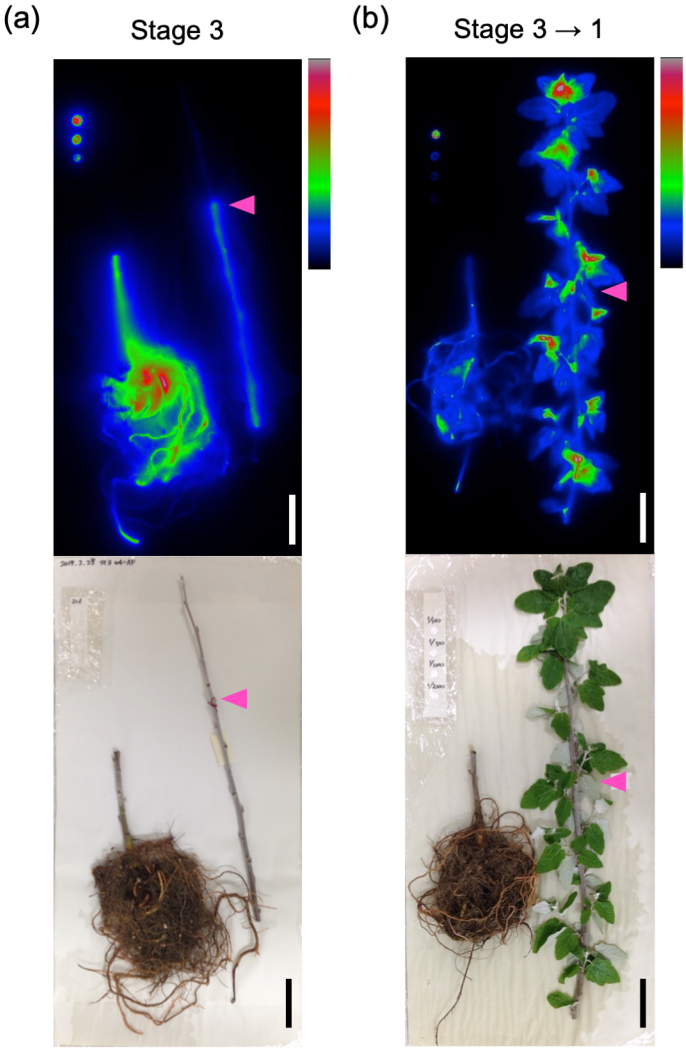

Fig. 6 Overview of the seasonal change of P re-translocation in *Populus alba*. In the growing season, P is mainly re-translocated from the 6th leaf to upper tissues (young leaves, apex) via phloem. P is re-translocated also to the axillary bud. During senescence, P is re-translocated from the 6th leaf to lower tissues (stem, roots) via phloem. P is exchanged from phloem to xylem near the 6th leaf, and accumulated in ray cells and perimedullary cells for winter storage.

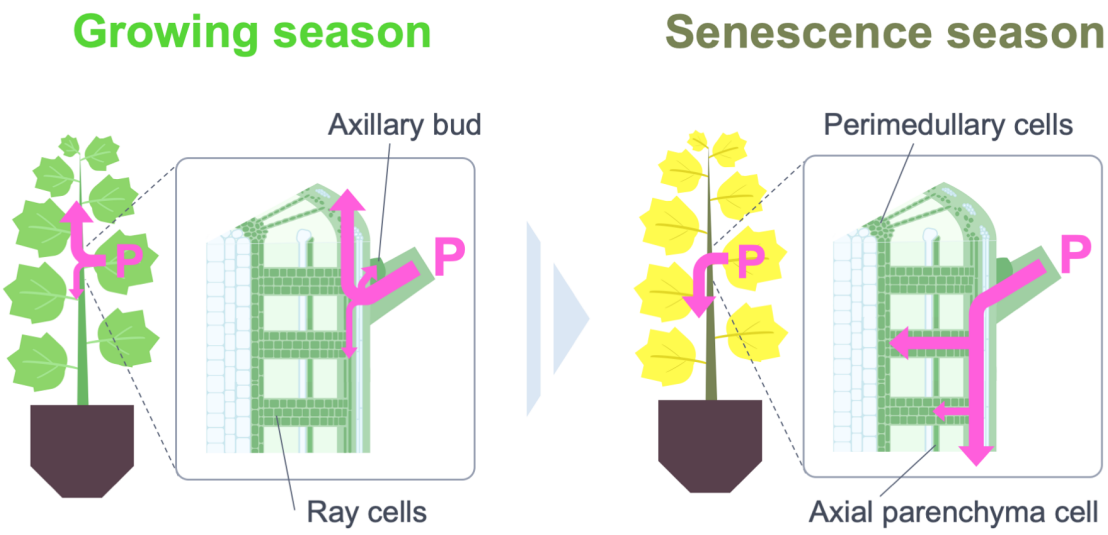

601 **Figure legends of Supporting Information**

602

603 **Fig. S1** Surgical treatments on *Populus alba* trees and a summary diagram of culture

604 conditions.

605 **Fig. S2** Transition of ^{32}P signal intensity (intensity cm^{-2}) of the apex and the 6th leaf axil.

606 **Fig. S3** ^{33}P autoradiographs of leaf axil of 6th leaf in stage 1 using imaging plate.

607 **Fig. S4** Microautoradiographs of the stem between 5th and 6th nodes.

608 **Video S1** Real-time imaging movie of ^{32}P in *Populus alba* at stage 1.

609 **Video S2** Real-time imaging movie of ^{32}P in *Populus alba* at stage 3.

610 **Video S3** 3D image of the 6th axil of *Populus alba* at stage 1.

611 **Video S4** 3D image of the 6th axil of *Populus alba* at stage 3.